Research Journal of Applied Sciences, Engineering and Technology 5(9): 2863-2869, 2013
DOI:10.19026/rjaset.5.4818
ISSN: 2040-7459; e-ISSN: 2040-7467

Submitted: February 05, 2013 Accepted: March 02, 2013 Published: March 20, 2013

Research Article

Environmental Influence on Automatic Landing Error of the Carrier-Borne Aircraft

Han Zhimin and Hong Guanxin
School of Aeronautic Science and Engineering, BeiHang University, Beijing, China

Abstract: The aim of this study is to analyze the movement model of aircraft carrier and stern flow model under the influence of marine sport. Also, we focus on the influence of marine sports and aft flow on the landing error of the carrier-borne aircraft under the guidance of the automatic landing system in different sea state level by numerical simulation and calculation. The analysis result is meaningful to the aircraft carrier due to the fact that environmental factors have a great influence on the error of carrier-borne aircraft landing on aircraft carrier, especially; marine sports and aft flow always affect the movement of an aircraft carrier and landing process of carrier-borne aircraft.

Keywords: Aft flow, automatic carrier landing system, marine sports

INTRODUCTION

Marine sports and aft flow in the environmental factor is the major disturbance factors causing the landing error. When aircraft carrier was affected by the storm in the sea, its traveling sports and perturbation motion will be six degrees of freedom motion and affect the position of the ideal landing point. Therefore, the aircraft carrier movement presents the characteristics of the random motion.

The aft flow of aircraft carrier is very complex and its characteristics include nonlinear, unsteady, randomness and so on. The active area of aircraft carrier is big and the marine climate is bad. When the carrier-borne aircraft approach landing, the aft flow behind the aircraft carrier is very disadvantageous to the airplane landing. The disturbance of a whirlwind is an important factor, because a whirlwind is stronger, the burble after ship is bigger. And the direction of whirlwind has a big impact on distribution characteristics of aft flow.

Mission objectives of ACLS (Automatic Carrier Landing System) is that fully automatic landing of carrier-borne aircraft on the deck of an aircraft carrier can be achieved under various weather conditions.

System structure schematic diagram of ACLS is shown in Fig. 1 (Huff and Kessler, 1978; Qidan *et al*., 2012; Zhu, 2009).

The system basic principle of ACLS is as follows. The deck movement of an aircraft carrier caused by the waves lead to the change of the ideal landing point, at this time, the change of the ideal landing point is carried on the filter through deck motion compensator (DMC). Then, deck motion compensation instruction and position information of carrier-borne aircraft are inputted the ship-borne instruction computer together and the instruction computer will combine the information and give the landing flight path/attitude instructions through control equation. In the meantime, the instructions are linked to the carrier-borne aircraft through the wireless data chain, at this time, Automatic Flight Control System (AFCS) on the aircraft and Approaching Power Compensation System (APCS) operate the altitude control and the accelerator separately, so that aircraft can fly according to track instruction.

The objective of the study is to analyze the movement model of aircraft carrier and stern flow model under the influence of marine sport. In addition, we analyze the influence of marine sports and aft flow on the landing error of the carrier-borne aircraft under the guidance of the automatic landing system in different sea state level by numerical simulation and calculation.

MATERIALS

The movement spectrum of an aircraft carrier at sea is typical narrowband process. The frequency generally do not change a lot with the state of motion and the range of frequency is between 0.2 rad/s and 0.8rad/s. Changes of the external conditions only can change the peak power, the peak and bandwidth and the form of the spectrum is almost unaffected. Therefore, a simplified fitting method can be found possibly and it gives the general form of the movement spectrum of an aircraft carrier at sea, using to analysis the actual frequency spectrum (Peng and Jin, 2001; Huixin *et al*., 2011).

The pitching frequency spectrum transfer function corresponding Fig. 2 is as follows:

Corresponding Author: Han Zhimin, School of Aeronautic Science and Engineering, BeiHang University, Beijing, China

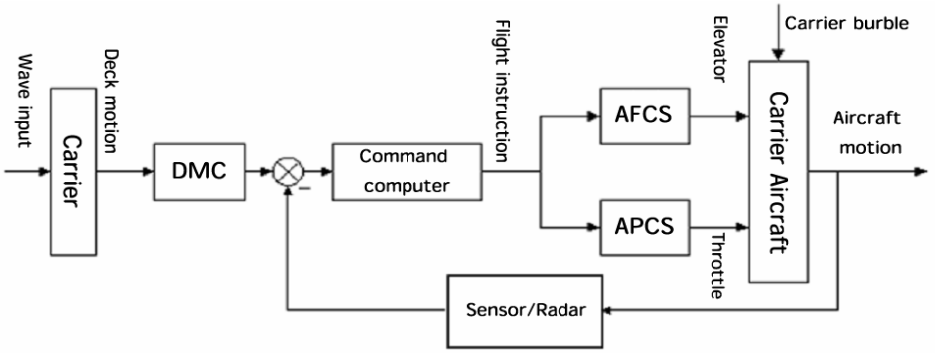

Fig. 1: System structure schematic diagram of ACLS

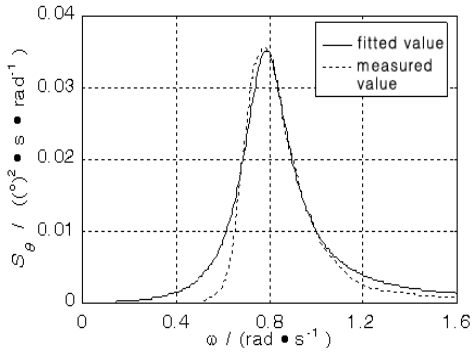

Fig. 2: Pitching frequency spectrum transfer function

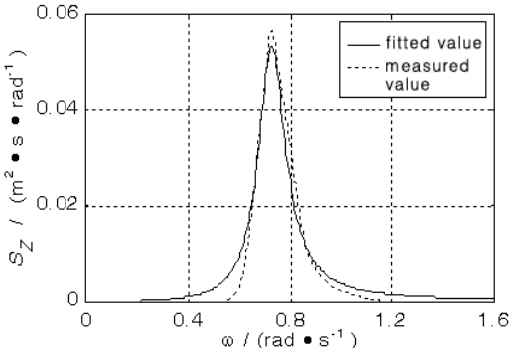

Fig. 3: Heave frequency spectrum transfer function

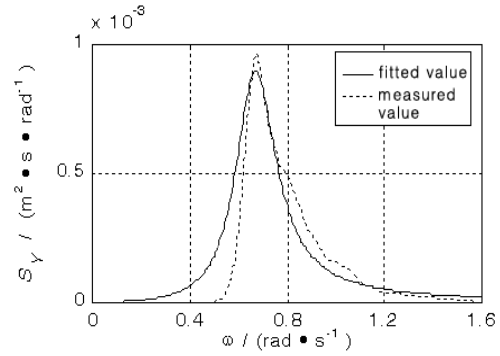

Fig. 4: Swaying frequency spectrum transfer function

$$G_\theta(s) = \frac{0.045s}{s^2 + 0.24s + 0.62} \tag{1}$$

The heave frequency spectrum transfer function corresponding Fig. 3 is as follows:

$$G_Z(s) = \frac{0.03s}{s^2 + 0.13s + 0.53} \tag{2}$$

The Swaying frequency spectrum transfer function corresponding Fig. 4 is as follows:

$$G_Y(s) = \frac{0.006s}{s^2 + 0.2s + 0.45} \tag{3}$$

The simplified fitting method using on movement spectrum of an aircraft carrier at sea is very intuitive and need the simple calculation process and small computation load. Therefore, it is a extremely practical and effective project method fitting narrow band stationary random process frequency spectrum.

THE METHOD

The disturbance velocity of aft flow model is composed as follows (Peng and Jin, 2000):

- Random free atmospheric turbulent flow u_1, v_1, w_1
- Steady-state disturbance of aft flow u_2, w_2
- Periodic disturbance caused by aircraft carrier movement u_3, w_3
- Random disturbance of aft flow u_4, v_4, w_4

The total atmospheric disturbance component is calculated as follows:

$$\left.\begin{aligned} u_g &= u_1 + u_2 + u_3 + u_4 \\ v_g &= v_1 + v_4 \\ w_g &= w_1 + w_2 + w_3 + w_4 \end{aligned}\right\} \tag{4}$$

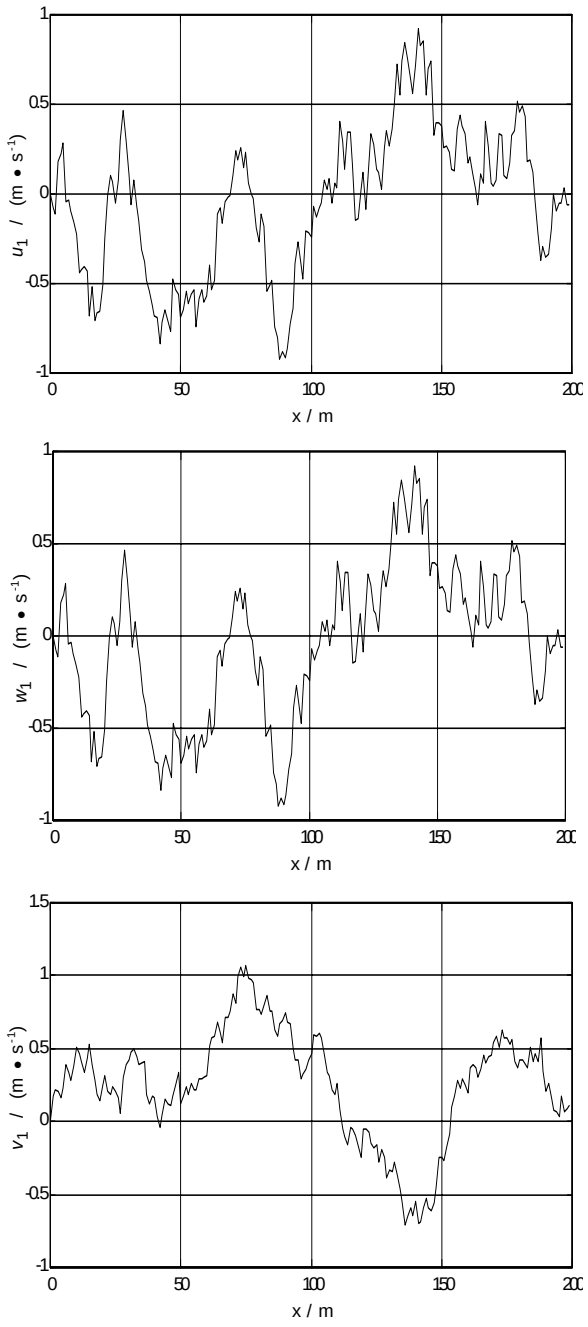

Fig. 5: Fragment of free atmospheric turbulence component at sea

u, v, w in the Eq. (4) is the components on the x, y, z axis of wind speed. The axis is defined that the x-axial to the front is positive, the y-axis to the right is positive and the z-axis to the under is positive.

Freedom atmospheric turbulence component at sea: The free atmospheric turbulence is the low-altitude free atmospheric turbulence component without the relative position of the aircraft and the aircraft carrier and it was anisotropic and its space power spectrum is as follows:

$$\left.\begin{aligned} S_u(\Omega) &= \frac{5.66}{1+(30.48\cdot\Omega)^2} \\ S_v(\Omega) &= \frac{26.59[1+(121.92\cdot\Omega)^2]}{[1+(304.8\cdot\Omega)^2][1+(40.64\cdot\Omega)^2]} \\ S_w(\Omega) &= \frac{2}{1+(30.48\cdot\Omega)^2} \end{aligned}\right\} \quad (5)$$

The units of the power spectrum in the Eq. (5) is $(m/s)^2/(rad/m)$, Spatial frequency is Ω and its units is rad/m.

When the numerical simulation results of the spectrum model were verified, the statistical characteristics such as root mean square and average value must be consistent with the theoretical value and also need to inspect whether the correlation coefficient and the power spectral density are consistent with the theoretical values.

A fragment of simulation result is shown in Fig. 5. It is the spatial distribution of free atmospheric turbulence component at sea u_1, v_1 and w_1 from top to bottom between 0 and 200 m and the origin of coordinates is the pitching center of an aircraft carrier here.

Steady-state disturbance of aft flow: Steady-state disturbance of aft flow is made up of static components of aft flow of aircraft carrier and is shown in Fig. 6. the horizontal component and vertical component is u^2 and w^2 and deck wind speed is Vwod in Fig. 6. The origin of coordinates is the pitching center of an aircraft carrier. And x forward is positive and backward is negative.

When the motion state of the aircraft carrier is constant, steady-state component of aft flow won't change. It also shows that the size of steady-state component of aft flow is decided by vow in Fig. 4.

Cyclical component of aft flow: Cyclical component of aft flow is produced due to the induction of the cyclical pitch and heave motions of the aircraft carrier. Along with the distance of the aircraft carrier pitching frequency, the pitching peak-to-peak value, the armor whirlwind as well as the carrier plane to the aircraft carrier changing and on a ship down lines of carrier-borne aircraft, it can be calculated as following formula:

$$\left.\begin{aligned} u_3 &= \theta V_{wod}(2.22+0.00295\cdot x)C \\ w_3 &= \theta V_{wod}(4.98+0.0059\cdot x)C \end{aligned}\right\} \quad (6)$$

In Eq. (6):

$$C = \cos\left\{\omega\left[t\left(1+\frac{V-V_{wod}}{0.85V_{wod}}\right)+\frac{x}{0.85V_{wod}}\right]+p\right\}$$

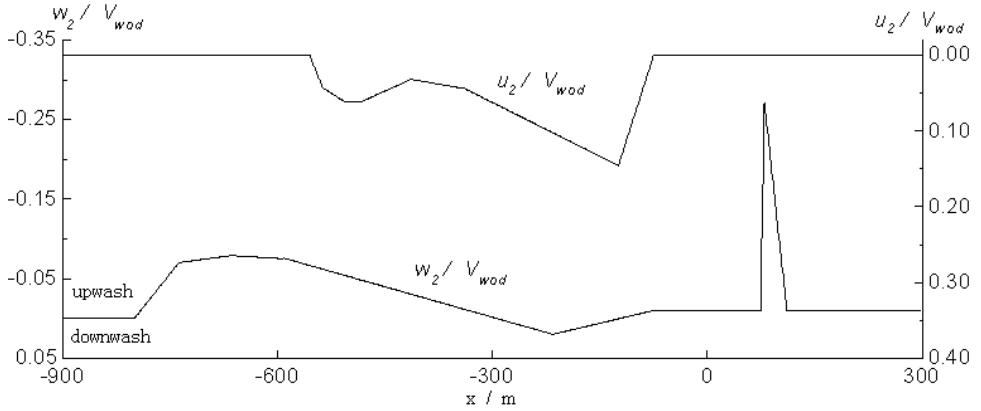

Fig. 6: Steady-state component of Aft flow

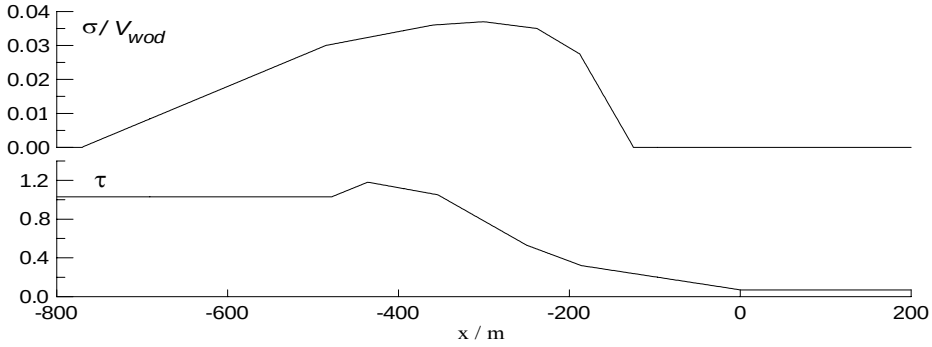

Fig. 7: $\tau(x)$ and $\sigma(x)$ of random turbulence component of aft flow

The level disturbance speed is u^3, m/s; Vertical disturbances speed is w^3, m/s; Pitching angular velocity of aircraft carrier is ωp, rad/s; Pitching amplitude of aircraft carrier is θ, rad; Deck wind speed is Vwod, m/s; Random phase is p, rad; x is the distance of the pitching center of the aircraft carrier and the direction of movement of the carrier is positive. When x<-681 m, component u^3 is zero; When x<-773 m, component w^3 is zero. Wind component is not given in Eq. (6) and it means that v^3 is zero.

Random turbulence component of aft flow: The turbulence is random atmospheric turbulence caused by the presence of the aircraft carrier. The power spectrum obtained by the measurement show that the atmospheric turbulence is anisotropic.

The filter calculation using the white noise is as follows:

$$\left.\begin{aligned} u_4 &= \frac{\sigma(x)\sqrt{2\tau(x)R}}{\tau(x)\,j\omega+1} \\ w_4 = v_4 &= \frac{0.035V_{wod}\sqrt{6.66R}}{3.33\,j\omega+1} \end{aligned}\right\} \quad (7)$$

In Eq. (7), R = [Pseudo-random number]

$$[\frac{j\omega}{j\omega+0.1}]\sin(10\pi t)$$

Deck wind speed is V_{wod}, m/s; The root-mean-square of random wake component is σ(x), m/s; Time constant is τ(x), s. With the change of the distance of the pitching center of the aircraft carrier, σ(x) and τ(x) will change, as shown in Fig. 7.

When simulating the turbulent flow components, according to the distance from the center of the aircraft carrier pitching to the location to be simulated, σ and τ are read. σ(x) will be obtained if σ multiplied V_{wod} and j_ω is replaced by Laplace operator s in Eq. (7). The random turbulence component model is became the form of the transfer function. At this time, σ(x) and V_{wod} are substituted transfer function, then, simulation will be carrying using the Simulink toolbox in matlab.

Guidance process simulation of ACLS: Based on the simulation of natural characteristics of the aircraft and control system and according to the physical image of F/A-18A landing and the work of ACLS (Prickett and Parkes, 2001), the simulated program of final ship error

is established and calculated. In the time domain, the entire quantity value simulation is carried and erroneous result of actual ship is analyzed.

MATLAB is a huge CACSD (Computer-Aided Control System Design) tool package, which contains a large number of numerical simulation of the control system algorithm and has been optimized and standardized processing, including transfer functions, systems of equations of state and other forms of numerical simulation.

Depending on the expected flying time, the landing engage time can be judged whether it is less than the 13s. If it is greater than 13s, DMC does not work and the height instruction is zero; otherwise, DMC is connected and according to the ideal position of the landing point, the height instruction compensated can be calculated.

The height instruction is transmitted to the flight control system. Then combined with the state parameters of flight and wind speed, output of autopilot/APCS is calculated and it is elevator input and throttle input of carrier aircraft. At this time, the flight state parameter of the next moment is calculated continually.

Through loop calculations, when the difference in height between the lowest point of the tail hook and aircraft carrier deck is zero, the loop ends. The final landing error can be calculated, it means that the horizontal distance between the aircraft landing engagement and the ideal landing point will be obtained.

EXAMPLE SIMULATION

Known as: aircraft speed is 69.96m/s glide angle is -3.5° deck wind speed is 12.86m/s time delay is 0.2s (Urnes and Hess, 1985)

The distance between every two block cable of NIMIZ aircraft carrier is 12 m. If the mid-point of the block cable 2 and the block cable 3 is looked as the Ideal landing point, the aircraft is linked to the point in the range of 18 m around the ideal landing point for a safe landing. In the Fig. 8 to 11, at the different sea conditions and under the influence of the aircraft carrier movement and aft flow Separately, distribution map of the airplane ship is obtained, through 50 times simulation.

- **Three-level sea state**
- **Six-level sea state**

CONCLUSION

- According to Fig. 8 and 10, data of the aircraft carrier movement influencing the Landing standard deviation can be obtained under different sea conditions. Effect of aircraft carrier under different sea conditions is shown as Table 1.

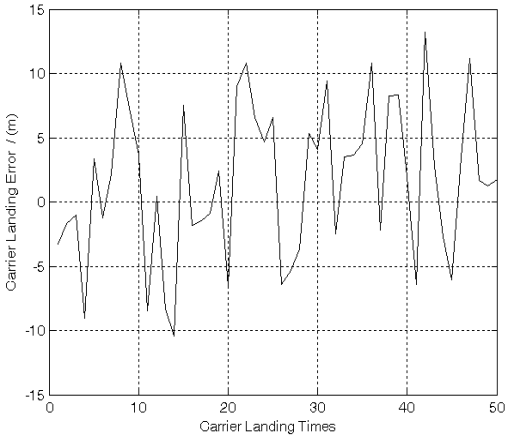

Fig. 8: Landing error under the influence of ship motion at three-level sea state

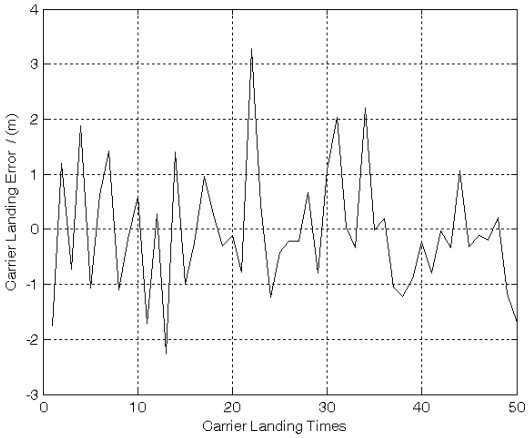

Fig. 9: Landing error under the influence of aft flow at three-level sea state

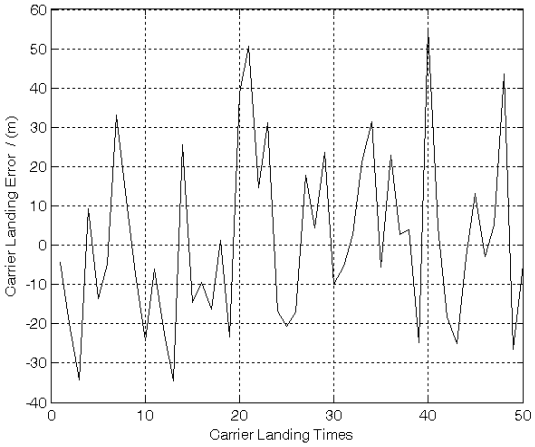

Fig. 10: Landing error under the influence of ship motion at six-level sea state

Table 1: Effect of aircraft carrier under different sea conditions

Sea state	Landing S.D (m)	Probability of landing success
Three-level	4.93	100%
Six-level	22.78	54%

Table 2: Effect of aft flow under different sea conditions

Sea state	Landing S.D (m)	Probability of landing success
Three-level	1.12	100%
Six-level	7.49	78%

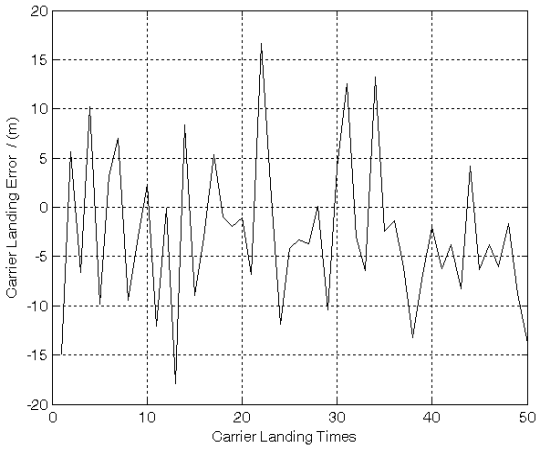

Fig. 11: Landing error under the influence of aft flow at six-level sea state

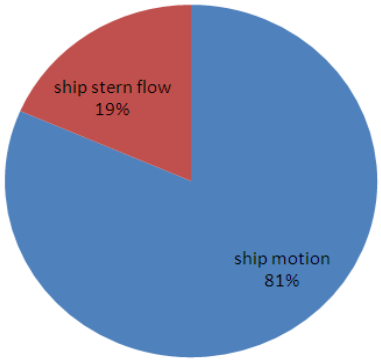

Fig. 12: Comparison of carrier movement and aft flow under three-level state

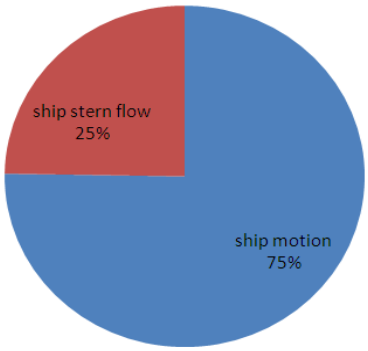

Fig. 13: Comparison of carrier movement and aft flow under six-level state

With the level of sea state increasing, the movement amplitude of aircraft carrier increases. Under the three-level sea state and the guidance of fully automatic landing guidance system, carrier-based aircraft can land 100% safely; under the six-level sea state, due to vice-value increasing and frequency changing fast of aircraft carrier movement, when the automatic landing guidance system track ideal landing point, the response has the bad trajectory control stability and other reasons and the landing error will increase, in the meantime, random insecurity factors will increase and makes the probability of successful landing reduce.

- According to Fig. 9 and 11, data of aft flow influencing the Landing standard deviation can be obtained under different sea conditions. Effect of aircraft carrier under different sea conditions is shown as Table 2.
  With the level of sea state increasing, effect of aft flow also increases. Under the three-level sea state, landing success rate is100%; under the six-level sea state, strength of aft flow increases and it makes landing success rate reduce to 78%.
- From Table 1 and 2, we can see that the impact of the landing error of the aircraft carrier movement is greater than the aft flow's. Under the three-level sea state and six- level state, the landing error of the aircraft carrier movement and aft flow is as shown in Fig. 12 and 13.

Under different sea states, the impact of the automatic landing error of the aircraft carrier movement is greater than the aft flow's. Seen from Fig. 12 and 13, the landing error of the aircraft carrier movement is 3 to 4 times than the aft flow's. Therefore, the establishment of a fully automatic landing guidance system focus on considering to eliminate landing error of the aircraft carrier movement.

REFERENCES

Huff, R.W. and G.K. Kessler, 1978. Enhanced Displays, Flight Controls and Guidance Systems for Approach and Landing. AD/A244 869. Retrieved from: http://www.dtic.mil/cgi-bin/GetTRDoc?AD=ADA244869&Location=U2&doc=GetTRDoc.pdf.

Huixin, T., L. Kun and M. Bo, 2011. A novel prediction modeling scheme based on multiple information fusion for day-ahead electricity price. Proceeding of the Chinese Control and Decision Conference (CCDC), pp: 1801-1805.

Peng, J. and C.J. Jin, 2000. Research on the numerical simulation of aircraft carrier air wake. J. Beijing Univ., Aeronaut. Astronaut., 26(3): 340-343.

Peng, J. and C.J. Jin, 2001. Simplified method to fit the power spectrum of narrow-band stochastic process. Acta Aeronaut. Astronaut. Sin., 22(3): 253-255.

Prickett, A.L. and C.J. Parkes, 2001. Flight testing of the F/A-18E-F automatic carrier landing system. Proceedings of the IEEE Aerospace Conference, pp: 2593-2612.

Qidan, Z., Y. Yongtao, Z. Zhi, Z. Wen and W. Zixia, 2012. Design of approach power compensation system for carrier-based aircraft using conditional integral sliding surface. Proceeding of the International on Information and Automation (ICIA), pp: 821-826.

Urnes, J.M. and R.K. Hess, 1985. Development of the F/A-18A automatic carrier landing system. J. Guid., 8(3): 289-295.

Zhu, Q., 2009. Adaptive variable structure guidance system design of a longitudinal automatic carrier landing system. Proceeding of Chinese Control and Decision Conference, pp: 4855- 4859.